Bull. Astr. Soc. India (2005) **33**, 103–108

Interpretation of angular diameter measurements of Mira variables : role of water*

A.Tej[1], A. Lançon[2] and M. Scholz[3]
[1] *Tata Institute of Fundamental Research, Mumbai 400005, India*
[2] *Observatoire Astronomique de Strasbourg, Strasbourg, France 67000*
[3] *Institut f. Theoretische Astrophysik der Universität Heidelberg, 69121 Heidelberg, Germany and School of Physics, University of Sydney, NSW 2006, Australia*

Abstract. For stars with atmospheres as complex as those of Miras, determination of fundamental stellar parameters remains a challenge. Occurrence of water "shells" and their implication on the interpretation of the angular diameter measurements will be discussed in this talk. The role of a spectrophotometric index of water in estimating the continuum diameter will be highlighted.

Keywords : Stars: fundamental parameters – Stars: late-type – Stars: variable: general – Stars: atmospheres

1. Introduction

Miras are pulsating variables undergoing rapid mass loss (10^{-7} – 10^{-6} $M_\odot$ yr $^{-1}$). Estimation of fundamental stellar parameters of these stars are crucial for understanding mass loss, pulsation and the late stages of stellar evolution. High angular resolution (HAR) techniques thus play an important role in studying Miras as they directly yield the angular diameter which is used in deriving the effective temperature and the linear radii of the star. Apart from this, a wealth of other important information regarding the Miras can be retrieved from HAR measurements. Geometry and structure of the stellar atmosphere, surface inhomogeneities and asymmetries, position of shock fronts, stellar mass are to name a few.

Over the last two decades there has been tremendous improvement in observational

*This talk is based on the published work - Tej et al., 2003, *A&A*,**401**, 347.

accuracies. Simultaneously, there has been substantial progress in theoretical modelling of Mira atmosphere. Despite this, defining a physically sensible radius (cf. Baschek et al., (1991) for a detailed discussion on various radii definitions) and interpreting the HAR measurements in terms of such a quantity is non-trivial for Miras owing to their geometrically extended and dynamic atmospheric configurations. Moreover, formation of deep molecular bands at substantially larger distances from the stellar centre makes it observationally challenging to probe and sample the 'real continuum'. In case of O-rich Miras, which are of interest to us, H_2O (besides CO) is the most abundant molecule in the stellar atmosphere and is also the dominant absorber in the near-IR with broad absorption features centered at 1.4, 1.9 and 2.7 μm. The wings of these broad features tend to contaminate the continuum radiation in the standard near-IR passbands (J, H, K and L). This is of major concern because generally HAR observations of these cool Miras are carried out in the near-IR as the spectral energy distribution of these variables peak in this wavelength zone.

Observationally, information about the physical dimension of the star is obtained from the brightness distribution across the stellar disk. The shape of the centre-to-limb variation (CLV) of emitted intensity across the stellar disk defines an 'intensity radius' which is translated via model considerations to a physically sensible 'optical-depth radius'. The most common optical-depth radius used in stellar theories is the Rosseland radius which marks the layer where the Rosseland mean opacity equals unity. Reconstructing the CLV to derive an intensity radius is not yet feasible with the present day interferometric techniques. Diameters are instead determined by comparing model-predicted visibility profiles (which are Hankel transformations of the CLVs) with the observed visibility profiles. Usually, a well defined uniform disk model is used which is far from reality for these extended configurations. A detailed summary of the present state of Mira science with interferometry can be found in a recent review by Scholz (2003).

2. Water "shells" in Mira atmosphere

Layers of high molecular density may often be considered as a "molecular shell" which is more or less detached from continuum-forming layers depending on the temperature and density stratification of the Mira atmosphere. Recent interferometric observations of Miras by Mennesson et al., (2002) show a strong increase in the measured UD diameter between the K' and the L' bands. These authors propose a two-layer scenario with a classical photosphere and a detached and extended ($\sim$ 3 stellar radii) gas layer to account for this chromatic variation in size. Similar two-layer models are also invoked by Yamamura et al. (1999) to model the ISO/SWS spectra of o Cet and Z Cas. A two-layer "slab" model with plane parallel uniform molecular layers of H_2O placed one above the other is shown to accurately fit the observed spectrum.

We investigate the presence of these water shells in time series of Mira models and their implication on the shape of the CLVs. We have used the models described in Bessell

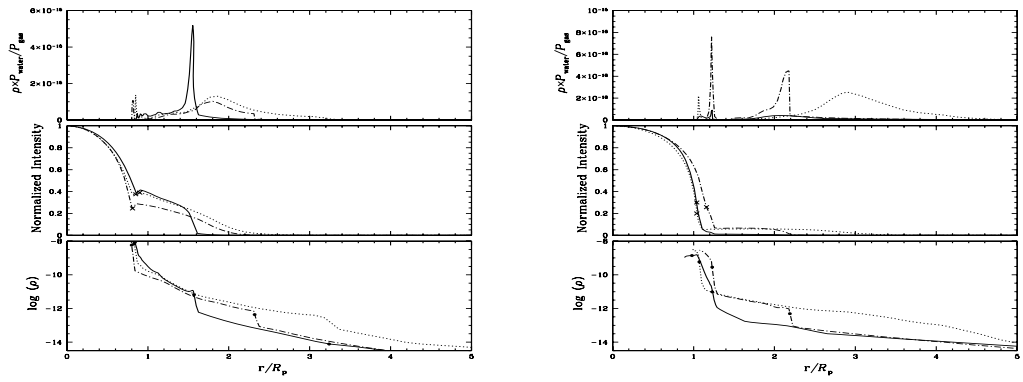

Figure 1. The relation between the the water "shells" (upper panel), the CLV shapes (middle panel) and the density structure (lower panel) for P model CLVs (left - near minima; right - near-maxima). In the middle panel the positions of the continuum-forming layer ($R_{1.04}$) are shown with crosses. In the lower panel the location of the shock fronts (computationally smeared out) are marked with filled circles. The line types are solid - P05 and P10; dotted - p15 and p20; dash-dotted - P35 and P40 respectively in the two plots. An abbreviated nomenclature (letter defining the series followed by the pulsation phase ($\times$10) is adopted for the model names.

et al., (1996) and Hofmann et al., (1998). Some new models were introduced in Tej et al., (2003). To display the shells, we use the quantity $\rho \times P_{water}/P_{gas}$, where P_{gas} is the total gas pressure and P_{water} the partial pressure of H_2O. It measures the density of water molecules. In Figure 1, we plot the near-minima and near-maxima P models. An abbreviated nomenclature (letter defining the series followed by the pulsation phase ($\times$10) is adopted for the model names. The upper panels show this shell parameter as a function of the radius, the middle panels plot the respective CLVs and the lower panels show the density structure for these models. Note that the computational smoothing of the shock fronts slightly affects the detailed behaviour of the corresponding areas in all panels.

The CLVs display two-component shapes consisting of a moderately darkened inner continuum portion and an outer tail-(for near-maxima) or protrusion-type(for near-minima) extension. The profile of the water shells clearly plays a role in defining the shape and strengths of the tail/protrusion component of the CLVs. For the protrusion-type P models, which occur during minima, the effective temperature is low and there is a steep density gradient after the position of the innermost shock front. Shells are formed relatively close to the continuum-forming layers. The extension of these shells depends significantly on the nature of propagation of shocks. The water shells for the tail-type P models are of different nature. These occur during maxima and for higher effective temperature. Tails correspond to shells with significantly lower water density than protrusion. The shells are detached from the continuum-forming layers and are located in higher atmospheric regions.

Apart from the very good one-to-one correlation seen between the water shells and the shapes of the CLVs, in general we see that the shells are detached and more extended for the tail-type models as compared to the protrusion-type ones. This is in gross agreement with the results of Yamamura et al., (1999) who surmise that H_2O layers are more extended at maxima. Mennesson et al. (2002) derive a photospheric radius of 10 mas and a H_2O envelope extending from 15 mas to 27 mas for R Leo. This "gap" of 1.5 $R_\star$ between the continuum layer and the H_2O envelope is in good agreement with the shells seen for the tail-type P models. Occurrence of such "gaps" is the natural consequence of the temperature-density requirement of the equation of state for H_2O formation.

3. Spectrophotometric signatures of visibility distortions

Jacob and Scholz (2002=JS02) show that the molecular-band contamination can distort visibility curves. Consequently, the fit diameter (by means of a UD or a fully darkened disk) is appreciably dependent on the spatial frequency (i.e. the baseline of observation). The choice of an appropriate atmospheric model and of the corresponding CLV is a critical step in the determination of a stellar diameter.

Water molecules are the main culprit of the two-component nature of the near-IR CLVs. Hence, we look for spectrophotometric features which would quantify the amount of water present in Miras. The H_2O index defined by Persson et al., (1977) and Aaronson et al., (1978) is a good indicator. It measures the ratio of the fluxes measured through narrow-band filters centered, respectively, in the wing of the 1.9 μm water band (λ = 2.0 μm) and in the K band (λ = 2.2 μm). The index is expressed in magnitudes and is zero for Vega. To quantify the strength of the tail/protrusion feature of the CLVs, we divide the CLV into two parts - the inner disk, and the tail- or protrusion- type extension. The ratio of the area of the extension with respect to the inner disk gives an estimate of the feature strength. We see a direct correlation between the strength of the CLV extensions and the H_2O index. The strength increases with the increase in the H_2O index.

However, the CLVs are not directly observable quantities but the shapes have a direct implication on the measured visibilities. JS02 have done a detailed study of the effects of phase, cycle and baseline on the measured continuum diameters of different Mira models. They fit UD visibility to the full model-predicted visibilities by means of a least square routine and also carry out single point fits of the UD to the model visibility at three spatial frequencies the choice of which covers the entire range of various model visibilities. The least square fitting to the full model takes care of the arbitrary choice of baselines and the three point fitting gives the baseline dependence of fitted diameters. The near-IR bands show substantial deviation of the fitted UD diameters from the near-continuum values. Apart from uncertainties of model treatment of molecular and dust opacities at very low temperatures, $R_{1.04}$ (the monochromatic radius defined at $\tau_{1.04} = 1$ in the 1.04 μm continuum window) is very close to the continuum value. We refer the reader to

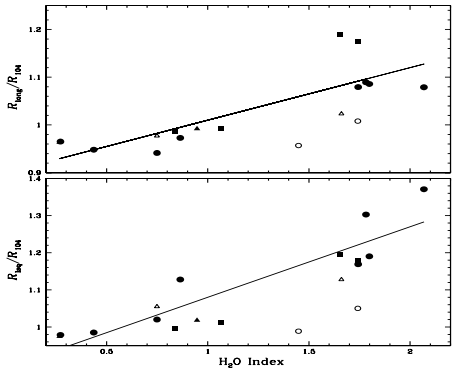

Figure 2. In this figure we plot the deviations of the UD fitted diameters from the the $R_{1.04}$ for the K band. The data points are taken from Figures 8,9 & 10 of JS02. The lower panel shows the results from the least squares and the upper panel shows the long baseline values. The symbols are P models - filled circles; D models - filled triangles; M models - filled squares; O models - open circles; E models - open triangles

JS02 for a detailed discussion of the points outlined above. As an obvious next step, we explore the correlation between the H_2O index and the deviations of fitted UD diameters from the continuum values. We use the K band results of Figures 8, 9 & 10 of JS02 for our study.

In the lower panel of Figure 2, we plot the ratio of the least squares fit UD radius ($R_{\rm lsq}$) to the near-continuum radius ($R_{1.04}$) as a function of the H_2O index. Although the dispersion is large, the deviations of the fitted UD diameters from the continuum values distinctly increases with water contamination. The relation tightens if the overtone models (O and E series) are left out. A linear least squares fit to the model points excluding the overtone models yields

$$R_{\rm lsq}/R_{1.04} = 0.19\ {\rm H_2O} + 0.89 \qquad (1)$$

In the upper panel we plot the correction factor for long baseline observations ($R_{\rm long}/R_{1.04}$). This baseline is positioned near the first null of the visibility function. It is more sensitive to the details of the CLV structure. The least squares fit to this gives

$$R_{\rm long}/R_{1.04} = 0.11\ {\rm H_2O} + 0.90 \qquad (2)$$

Similar trends are seen for the medium and short baselines (not plotted). The ratios of interferometric UD radii to the Rosseland radius R (instead of $R_{1.04}$) show much more scattered relations to the H_2O index. This is expected because of the nature of the Rosseland opacity which is a harmonic-type mean opacity and is sensitive to extended regions of strong molecular extinction which tends to close the near-continuum windows, to increase the Rosseland opacity and, hence, to increase the Rosseland radius as compared to the continuum radius. The above two linear fits emphasize the fact that a simultaneous

spectral observation of water contamination could yield a correction factor for deriving continuum diameters from the UD fitted values.

4. Conclusion

The models are shown to naturally produce water-rich shells depending on temperature and density stratification of the atmospheric models. The propagation of shock fronts plays a decisive role in the structure and extent of the shells and has direct effect on the shapes of the CLVs. The model-predicted strength of the H_2O index, quantifying the 1.9 μm water feature, gives a good indication of the nature of the CLV in terms of the strength of the tail/protrusion features with respect to the inner continuum disk. The increase in water contamination from the K band to the L band is evident from the increase in the feature strength for the L band CLVs.

Using the results of JS02, we show that the deviations of the fitted UD diameters from the continuum values are correlated with the H_2O index, though with a significant dispersion. The results are based on a moderate number of models covering a limited range of stellar parameters, phases and cycles, which prevents us from identifying the origin of the scatter. The exact form of this correlation still has to be determined from future high-precision visibility observations, and the usefulness of a simple linear approximation as given in Eqs. (1) and (2) still has to be checked both empirically and with more models. Until then, simultaneous spectroscopic observations of water bands may at least warn the interferometric observer and provide a rough estimate of corrections to be applied to the UD fit diameters.

References

Aaronson, M., Persson, S. E., and Frogel, J. A., 1978, *ApJ*, **220**, 442.
Baschek, B., Scholz, M., and Wehrse, R., 1991, *A&A*, **246**, 374.
Bessell, M. S., Scholz, M., and Wood, P. R., 1996, *A&A*, **307**, 481 (BSW96).
Hofmann, K.-H., Scholz, M., and Wood, P. R., 1998, *A&A*, **339**, 846 (HSW98).
Jacob, A. P., and Scholz, M. 2002, *MNRAS*, **336**, 1377. (JS02).
Mennesson, B., Perrin, G., Chagnon, G., Coudé du Foresto, V., and Ridgway, S. T., et al., 2002, *ApJ*, **579**, 446.
Persson, S. E., Aaronson, M., and Frogel, J. A., 1977, *AJ*,**82**, 729.
Scholz, M., 2003, in: Traub W.A. (ed) Astronomical Telescopes and Instrumentation 2002 - Interferometry for Optical Astronomy II, SPIE Conf. 4838, p.163.
Tej, A., Lançon, A., Scholz, M., 2003, *A&A*, **401**, 347.
Yamamura, I., de Jong, T., Cami, J., 1999, *A&A*,**348**, L55.